

# **Ball Shaped End-caps for Fiber Laser Systems**

Wenxin Zheng, Director of Engineering - Fusion Splicing Division, AFL Gongwen Zhu, Application Engineer, AFL

## **ABSTRACT**

End-caps of different types are widely used in fiber laser systems to reduce the fiber facet damage threshold and the back reflection. Most commercial end-caps consist of a cylindrical rod of fused silica with a flat or angle polished end-surface. By fusion splicing the end cap to the output fiber, the laser beam diverges and the spot size enlarges inside the end-cap. Thus, the power density at the air-silica interface is much lower compared to the case without end-capping. However, with the traditional cylindrical rod shape, the divergent beam angle exiting from the end-cap may not be desired, but will be the result due to the flat (or angled) end surface of the end-cap. For many applications (such as medical surgery, metal cutting, etc.), less divergent, collimated, or focused beams are required. Spherical shaped end-caps are developed to meet the requirements for lower back-reflection, higher reliability, and flexible beam (convergent or divergent) angle. In this paper, general ball shaped end-caps are studied and illustrated. Different ball shaped end-caps were tested and measured for a variety of applications. For example, a 2.2 mm diameter ball shaped end-cap was manufactured on the end of the output LMA fiber and tested with a 1.7 kW fiber laser system.

**Keywords:** Ball lens, end-caps, fiber laser, fusion splicing, CO<sub>2</sub> laser splicing

#### 1. INTRODUCTION

High power and ultra-high power fiber lasers were developed in recent decades for many applications. [1] Fiber lasers with output power levels up to 100 kW were developed a few years ago. [2] The fiber end-surface will be easily damaged at the silica-air facet by the very high power density. A variety of cylindrical fused silica end-caps have been developed for high power fiber laser systems to reduce the power density at the silica-air facet. [3] Many different methods and equipment have also been created for making and splicing those cylindrical shaped end-caps. [4] [5] In the current fiber laser research institutes and industry, cylindrical shaped end-caps with anti-reflection (AR) coating and/or angle polished facet are almost the only choice for fiber termination.

The most important requirements for end-caps are low back reflection to the fiber core and cladding, reliability of end-cap facet, and flexible beam propagation properties from the end-cap facet, such as collimated or converging beam shapes instead of only a diverging beam (which is a typical limitation with cylindrical end-caps). An uncoated flat facet cylindrical end-cap normally has -35 dB back reflection to the core and -16 dB to the cladding. With AR coating, the back reflection can be reduced by about 10 dB, to a level of -45 dB to the core and -26 dB to the cladding respectively. With a 5-to-8 degree end-face polish angle, the level of reflection can be further reduced to -55 dB and -35 dB. [6] The process for cylindrical end-cap manufacturing normally involves three steps; (1) cleaving or polishing a glass rod, (2) deposit an AR coating with a special oven, and finally (3) splice the end-cap to the output fiber. The entire process is normally tedious and costly. At high power output the laser damage threshold of the AR coating becomes a concern. The damage threshold for an uncoated fused silica is about eight times higher than AR coated samples. [7] For making a collimated or converging beam with a conventional end-cap, tests were reported by heating the output surface with a H<sub>2</sub>-O<sub>2</sub> flame to form monolithic collimators. [8]

In this paper, ball shaped end-caps will be introduced, investigated, and discussed. A set of general formulas for back reflection computation are derived with cylindrical end-caps in Section 2. The computation for spherical end-caps is discussed in Section 3. Beam propagation from the spherical end-caps is further explored in Section 4. The process for manufacturing ball shaped end-caps, beam quality measurement, and high power test results are introduced in Section 5. Some concluding remarks are provided in Section 6.



## 2. BACK REFLECTION FROM CYLINDRICAL END-CAPS

Figure 1 illustrates the dimensions and characteristics required for the analysis of the back reflection from a cylindrical shaped end-cap. An output fiber having cladding diameter  $d_1$  from a fiber laser system is spliced to an end-cap with length L and diameter  $d_2$ . The output fiber is either single-mode fiber (SMF) or large mode area fiber (LMA). The LP01 mode carried by the output fiber can be approximated by a Gaussian beam. Its beam diameter at  $1/e_2$  of the peak power is equal to the fiber mode field diameter (MFD) and is denoted as  $2w_0$ . Due to the lack of the fiber core in the end-cap, the beam diverges as it travels through the end cap resulting in a larger spot size. At the end of the end-cap, the spot size becomes  $2w_1$ . The divergent angle  $\theta$  can be computed by  $\theta = NA/n_2$ , where NA is the numerical aperture of the output fiber, and  $n_2$  is the refractive index of the end-cap material. Due to the Fresnel reflection at the air-glass surface, 4% of the total power will be reflected back at the end of the end-cap with the same divergent angle  $\theta$ . When the reflected Gaussian beam reaches the splice point, the spot size becomes  $2w_2$ .

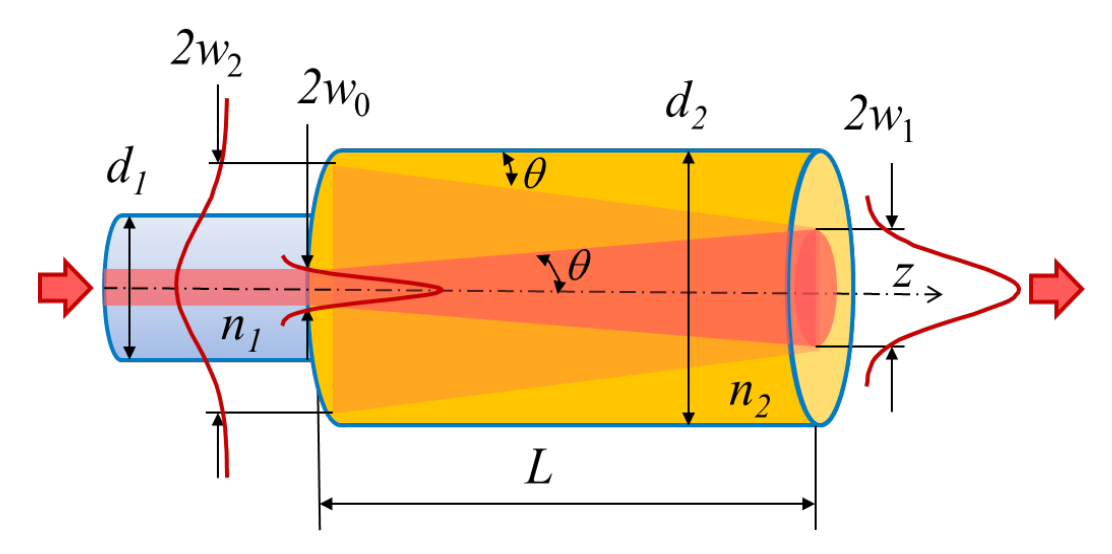


Figure 1 — Cylindrical end-cap with length L is spliced to an output fiber of a fiber laser system. The output fiber cladding diameter is  $d_1$ . The end-cap diameter is  $d_2$ . The beam divergent angle  $\theta = NA/n_2$ , where NA is the numerical aperture of the output fiber, and  $n_2$  is the refractive index of the end-cap material. The LP01 mode from the output fiber can be approximated by a Gaussian beam with mode field diameter denoted by  $2w_0$ . The diameter of the diverging Gaussian beam at the end of the end-cap is  $2w_1$ .

The diameter of the back reflected beam at the splice point is  $2w_2$ .

The Gaussian beam intensity in the end-cap can be expressed as

$$I(r,w) = I_0 e^{\frac{-2r^2}{w^2}} \tag{1}$$



Where r is the radius from the beam propagation axis z, w(z) is a function of z, and  $I_0$  is the peak intensity of the beam at z = 0. Thus the power propagating through any circle centered at the beam axis with radius r can be obtained by integration of the intensity.

$$P(r,w) = \int_0^{2\pi} \int_0^r I(r,w) r dr d\vartheta = P_0 (1 - e^{\frac{-2r^2}{w^2}})$$
 (2)

By defining the splice point as z = 0,  $w(0) = w_0$ , and  $2w_0 = MFD$  of the output fiber, the output power from the fiber, the reflected power from the end-cap surface to the splice can then be written in the following forms:

$$P_{out} = P(r \to \infty, w) = P_0, \ P_{core} = P_0 F\left(1 - e^{\frac{-2w_r^2}{w_2^2}}\right), \ P_{clad} = P_0 F\left(1 - e^{\frac{-d_1^2}{2w_2^2}}\right)$$
 (3)

The Fresnel coefficient F at the glass-air surface is known as F = 4% and the radius of the receiving aperture  $wr = n_1 w_0$ . Since the end-cap length L is much larger than the Raleigh range for most of the end-cap designs, the far field approximation can be used to obtain  $w_2 = 20$  L. Thus the back-reflection ratios for the core modes and cladding modes can be obtained as follows:

$$B_{core} = \frac{P_{core}}{P_{out}} = F\left(1 - e^{\frac{-2w_r^2}{w_2^2}}\right), \quad B_{clad} = \frac{P_{clad}}{P_{out}} = F\left(1 - e^{\frac{-d_1^2}{2w_2^2}}\right)$$
(4)

The return loss of core and cladding can then be calculated by

$$L_{core} = 10 \log \left[ F \left( 1 - e^{\frac{-2w_r^2}{w_2^2}} \right) \right], \quad L_{clad} = 10 \log \left[ F \left( 1 - e^{\frac{-d_1^2}{2w_2^2}} \right) \right]$$
 (5)

As one example, a double clad fiber (20/400 LMA with NA = 0.06/0.46) is spliced to an end-cap with L = 4 mm and  $d_1 = 0.4$  mm. Assuming  $n_1 \approx 1.5$ ,  $wr = n_1w_0 = 15$  µm,  $w_2 = 2\theta$   $L = 2\times0.06\times4000/1.5 = 320$  µm. From Equation (5), we can calculate  $L_{core} = -37$  dB and  $L_{clad} = -16$  dB. With a properly wavelength matched anti-reflection (AR) coating, the Fresnel coefficient can be reduced to F = 0.2%. Thus  $L_{core}$  can be reduced to -50 dB and  $L_{clad}$  reduced to -30 dB. These calculated return loss results agree well with the end-cap design software reported in Equation [6].

For actual measurement verification, 14 end-caps were spliced to Corning SMF-28e fibers and return losses were measured at 1550 nm using a JDS back-reflection meter. The end-caps with  $L=750~\mu m$  and  $d_2=125~\mu m$  were made using coreless fused silica fiber (Nufern FUD-3582). The computed return loss using Equation (5) is  $L_{core}=-36.8$  dB without AR coating, and -46 dB with 0.5% AR coating. The measured average return-loss is -35.5 dB without AR and -44.8 dB with AR, respectively. The calculated values agree well with the measured results. However, the computed back reflection is slightly lower than the measured values since we only consider the fundamental mode and one order reflection in our theoretical model. The multiple reflections inside the end-cap are not considered.

In the fiber laser industry, for a very high power output the AR coating is considered to be the weakest point to survive the high temperature and therefore limits long time reliability. Angle polished (or cleaved) end-caps can reduce the reflection without using AR coating. However, the output beam path will be diverted and the beam shape will be deformed by the polish angle at the end surface. The process of angle polishing also adds complexity and cost to end-cap manufacturing.



# 3. BACK REFLECTION FROM SPHERICAL END-CAPS

For reduction of back reflection without using AR coating, end-caps with spherical shaped or hemi-spherical shaped end surfaces are considered. For an analytic consideration, the important parameters are shown in Figure 2. For an easy comparison, similar notations are used for both Figure 1 and Figure 2. The end cap illustrated in Figure 2 consists of two sections: the cylindrical section which is similar to the end-cap in Figure 1, and the spherical section. The spherical end is generated by heating and pulling a coreless silica fiber (which has already been spliced to the output fiber) in order to break it off at the required length, followed by a second heating process to generate the spherical end shape. With a controlled heating process, the end of the coreless fiber melts and forms a perfect ball due to surface tension while the fiber is rotated to nullify gravitational effects which might otherwise deform the shape of the ball.

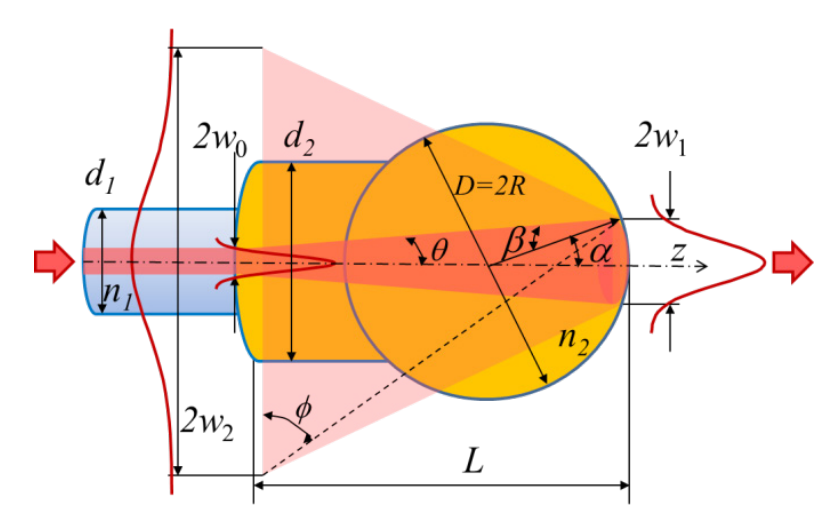


Figure 2 — Spherical end-cap with length L is spliced to an output fiber of a fiber laser system. The output fiber cladding diameter is  $d_r$ . The end-cap diameter is  $d_z$  and the diameter of the spherical end surface is D. The beam divergent angle  $\theta = NA/n_z$  where NA is the numerical aperture of the output fiber, and  $n_z$  is the refractive index of the end-cap material. The LP01 mode from the output fiber can be approximated by a Gaussian beam with mode field diameter denoted by  $2w_o$ . The diameter of the diverging Gaussian beam at the end of the end-cap is  $2w_r$ . The diameter of the back reflected beam at the splice point is  $2w_r$ .

With similar analytic derivation, Equation (5) is also valid for the spherical end-cap. However, the  $w_2 = 2\theta L$  is no longer valid for the spherical surface. To calculate  $w_2$ , new angles  $\alpha$ ,  $\beta$ , and  $\theta$  are introduced and shown in Figure 2. From a geometric analysis and the law of sines, the following relation can be derived.

$$\alpha = \phi + \beta \tag{6}$$

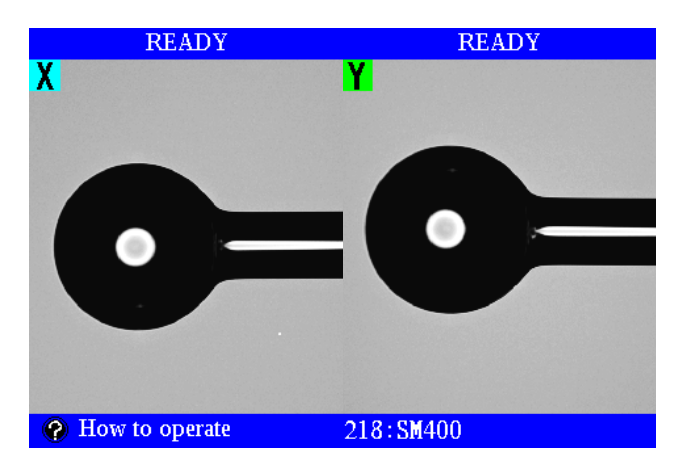
$$\phi = \frac{\pi}{2} - \theta - 2\beta \tag{7}$$

$$\sin \beta = [(2L - D)\sin \theta]/D \tag{8}$$

$$w_2 = (D\sin\alpha\sin2\beta)/(2\sin\theta\sin\phi) \tag{9}$$



By introducing Equation (9) into Equation (5), the return losses can be obtained for a spherical end-cap. To verify the analytic formulas, one ball shaped end-cap was made with the same material and similar dimensions to the end-cap described under Equation (5). A double clad fiber (20/400 LMA with NA = 0.06/0.46) was spliced to a coreless silica rod with  $d_2 = 0.4$  mm. After a D = 1000 µm ball was formed on the end of the silica rod, the total length from the splice to the ball tip is L = 3650 µm as shown in Figure 3. From Equation (5), the return loss to the core is calculated  $L_{core} = -52$  dB. The measured average return loss for this ball shaped end-cap at 1310 nm and 1550 nm is -51 dB. Again, the calculated back reflection is slightly lower than the measured value, due to the fact that multiple reflections were not considered as discussed previously.



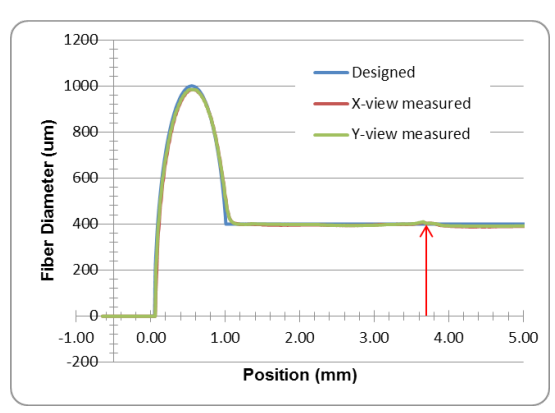
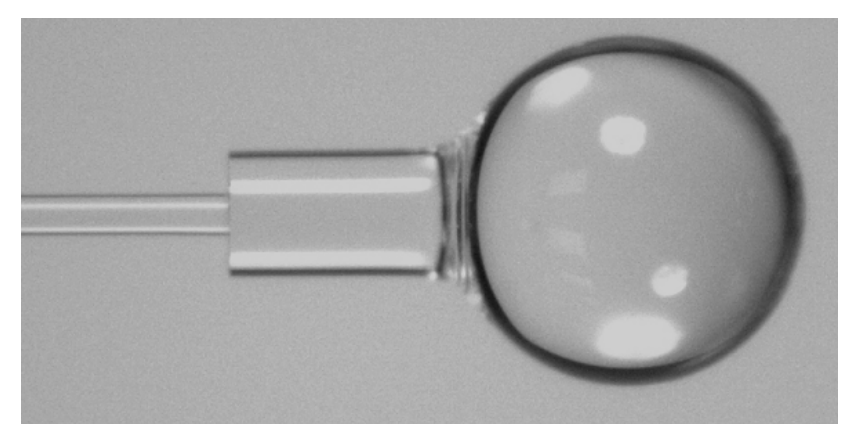


Figure 3 — A double clad fiber (20/400 LMA with NA = 0.06/0.46) was spliced to a coreless silica rod with  $d_2$  = 0.4 mm. After a D = 1 mm ball was formed on the end of the silica rod, the total length from the splice to the ball tip is L = 3.65 mm.

Another ball shaped end-cap was made with  $d_1 = 80 \mu m$  Corning RCSMF by MFD expansion spliced to  $d_2 = 250 \mu m$  coreless fiber (Nufern FUD-3432). A ball lens of  $D = 679 \mu m$  was formed as the end surface. The total length is  $L = 1140 \mu m$ . The calculated return loss is -36 dB while the actual measured value is -34 dB. A microscope photograph of this ball shaped end-cap is shown in Figure 4.



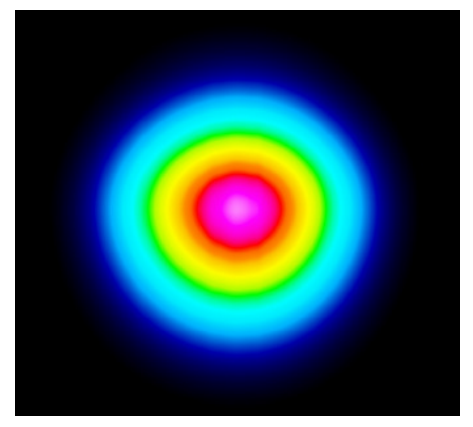
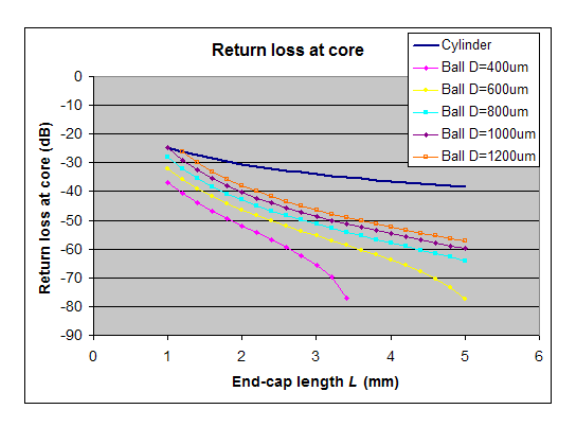


Figure 4 — A spherical end-cap was made of 80  $\mu$ m RCSMF with 250  $\mu$ m coreless fiber ( $D=679~\mu$ m,  $d_{_1}=80~\mu$ m,  $d_{_2}=251~\mu$ m,  $L=1140~\mu$ m). The beam shape was measured at the waist at  $\lambda=1550~\rm nm$ .



From the two examples above, we can clearly observe that the back reflection is not only a function of end-cap length L, it is also strongly dependent on the ball diameter. To gain an understanding of this dependence,  $L_{core}$  and  $L_{clad}$  of spherical end-caps with multiple ball diameters D and total lengths L were computed based on the fiber pairs shown in the example in Figure 3. The computed results are plotted in Figure 5. For comparison, the conventional cylindrical end-cap with the same length L is shown in the blue curves. From the charts, we can see that all return losses of the spherical end-caps are lower than that by cylindrical end-caps with the same length L. The return losses of the cylindrical end-caps are actually the upper limit when the ball diameter goes to infinity. By properly designing the geometry, the back reflection can be 10 dB to 30 dB lower than that from the cylindrical end-caps without AR coating. However, to achieve lower return loss is not the only goal for the end-cap design. The geometry of a spherical end-cap also needs to be optimized for the desired beam propagation beyond the end surface of the end-cap.



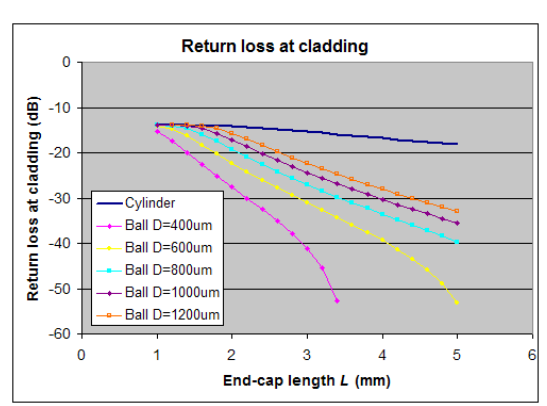


Figure 5 — Computed return losses at core (chart on left) and at cladding (chart on right) for spherical end-caps made with the same material and structure listed in Figure 3. The return losses of conventional cylindrical end-caps with similar design are also plotted and shown in the blue curves for comparison.

#### 4. BEAM PROPAGATION FROM SPHERICAL END-CAPS

For analysis of beam propagation, in Figure 6, a spherical end-cap is shown with similar notations as used for Figure 2. Different from cylindrical end-caps (which have only diverging beam propagation), the spherical end-cap can provide diverging, converging, or collimated beam propagation based on the end-cap design. Similar to our study for back reflection, Gaussian beam approximation is used since the considered beam propagation range is much larger than the Rayleigh range  $Z_R$ , where  $Z_R = \pi w_0^2/\lambda$ .



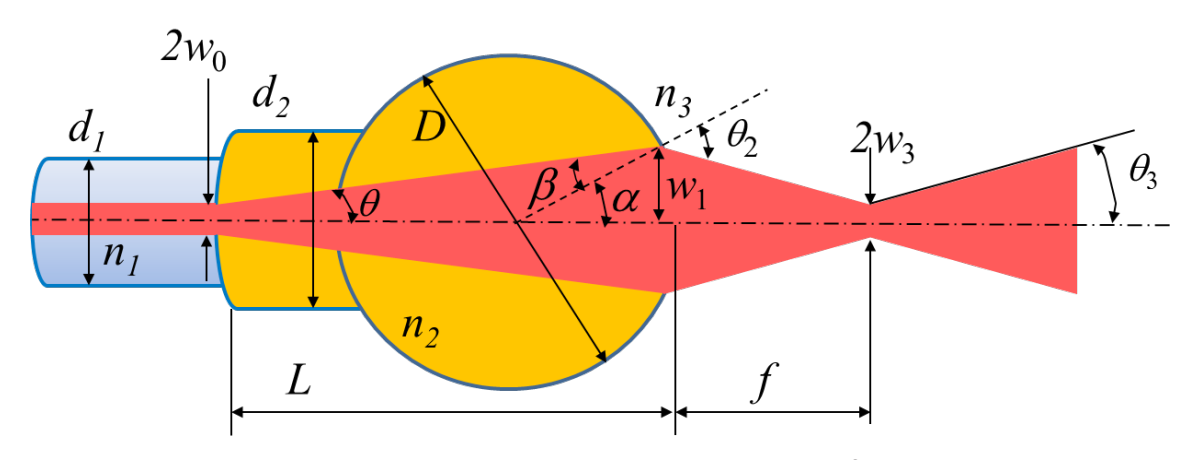


Figure 6 — Spherical end-cap with length L is similar to that shown in Figure 2. The output fiber cladding diameter is d₁. The end-cap silica rod diameter is d₂ and the diameter of the spherical end surface is D. The beam divergent angle inside the end-cap is  $\theta = NA/n_2$ , where NA is the numerical aperture of the output fiber, and n₂ is the refractive index of the end-cap material. A Gaussian beam approximation is used with beam diameters  $2w_0$  and  $2w_1$  at the end-cap input and output or surfaces, and  $2w_3$  at the waist of the propagated beam if the beam converges. The beam converging angle and propagation angle are denoted as  $\theta_2$  and  $\theta_3$ , respectively. The waist length f is the distance from the ball tip to the waist of the beam if it converges.  $f \to \infty$  for a collimated beam.

With geometric analysis and the Snell's law, the propagation angle  $\theta_3$ , waist length f, and beam waist spot diameter can be calculated analytically:

$$\theta_3 = \theta_2 - \alpha \tag{10}$$

$$\sin \theta_2 = n_2 (2L - D) \sin \theta / n_3 D \tag{11}$$

$$w_3 = \lambda/\pi\theta_3$$
 For  $\theta_3 > 0$  (12)

$$f = (w_1 - \sqrt{2}w_3)/\theta_3 + Z_R - D(1 - \cos\alpha)/2 \qquad \text{For } \theta_3 > 0$$
 (13)

Equations (12) and (13) are valid only if the beam is converging, i.e.,  $\theta_2 > \alpha$ . When  $\theta_2 = \alpha$ , i.e.  $\theta_3 = 0$ , the beam is collimated theoretically. Thus the collimation condition can be derived from Snell's law,  $n_3 \sin \alpha = n_2 \sin \beta$ , and Equation (8), we have

$$n_3 w_1 = n_2 (L - R) \sin \theta \tag{14}$$

Considering  $\sin\theta \approx \theta$  for small NA of a single-mode or a few mode fibers, the collimation condition can be written as

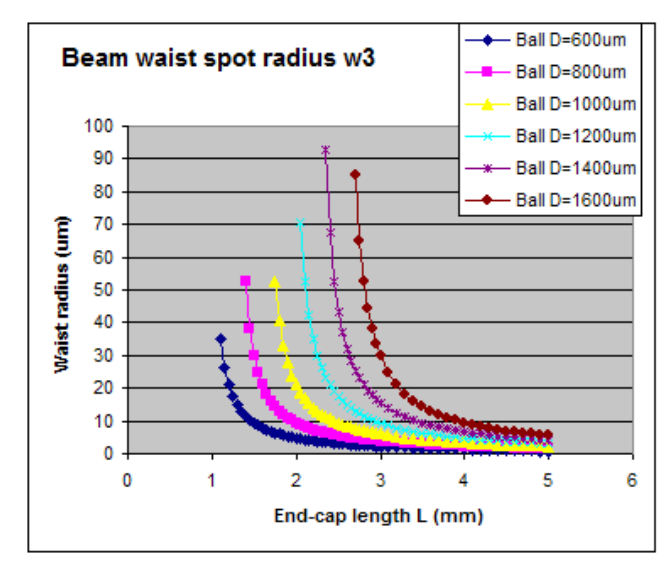
$$D \approx 2L(1 - n_3/n_2) \tag{15}$$



For fused silica and air,  $n_2 = 1.45$  and  $n_3 = 1$ , if the spherical end-cap meets  $L \approx 1.6D$ , the propagated beam in the air will become collimated. However, this collimation condition Equation (15) does not work for multimode fibers since the fiber NA is too big to meet  $\sin \theta \approx \theta$ .

The waist diameter and waist length expressed by Equations (12) and (13) have been validated by measurement of actual spherical end-caps made in our lab. To achieve a near collimated ball lens pair for SMF-28 non-contact connectors, three samples were made by splicing the SMF-28 to 125  $\mu$ m coreless fiber and forming a ball of R=355  $\mu$ m with end-cap length L=1290  $\mu$ m. The computed waist diameter and waist length are  $2w_3=38$   $\mu$ m and f=4.46 mm, while the average measured waist length is f=4.5 mm with 0.5 dB transmission loss between the ball lens pair. As a second example, more than 100 spherical end-caps were made using AFL RRSMFB radiation resistant single-mode fiber spliced to 125  $\mu$ m coreless fiber and forming a ball of R=225  $\mu$ m with L=850  $\mu$ m. The measured average waist FWHM spot is 21  $\mu$ m and focus 2.3 mm. The computed corresponding values are 20.5  $\mu$ m and 2.36 mm using Equations (12) and (13).

Below, the waist diameters  $2w_3$  and the waist lengths f of spherical end-caps with multiple ball diameters D and total lengths L were computed based on the fiber pairs shown in the Figure 3 example. The computed results are plotted in Figure 7. Theoretically, when the end-cap length L approaches the collimation limit 1.6D, the waist radius  $w_3$  approaches  $w_1$  and the waist length goes to infinity. Practically, it is not a good idea to design an end-cap very close to the collimation limit since the product performance will be inconsistent due to sensitivity to mechanical tolerances and environmental perturbation. On the other hand, for a very long end-cap, the diameter of the coreless fiber  $d_2$  has to be considered to ensure that the divergent beam does not touch the side wall.



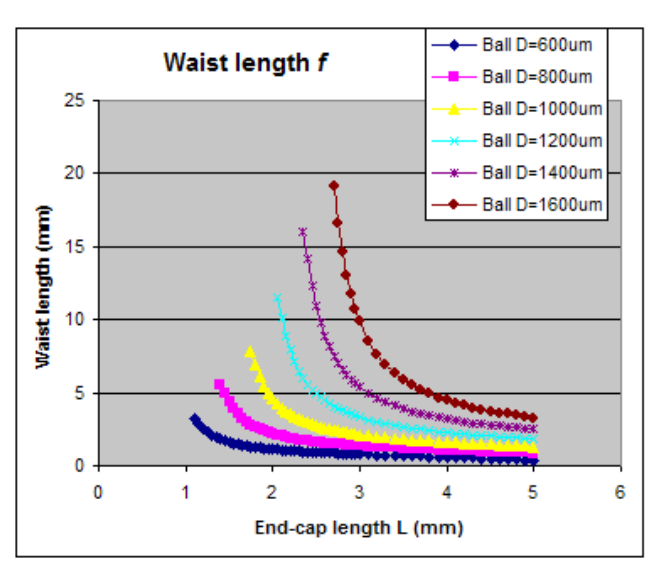


Figure 7 — Computed beam waist radius (left chart) and waist length (right chart) for spherical end-caps made with the same material and structure listed in Figure 3. The collimation happens at L = 1.6D, where the spot size grows to reach  $w_3 = w_1$  and the waist length goes to infinity.



#### 5. SPHERICAL END-CAP MANUFACTURING AND EXPERIMENTS

As discussed in previous sections, the beam guidance by the fiber core has to be clearly terminated at a defined location to achieve consistent spot size, waist length, and return loss by a well-defined L. This means that the spherical end-cap has to be made by splicing a piece of coreless fiber onto the transmission fiber and then forming the ball on the coreless fiber (instead of generating the ball directly on the end of the transmission fiber). A process for splicing the coreless fiber, breaking the coreless fiber, and forming a ball on the coreless fiber all in one automated sequence has been developed using the AFL/Fujikura LZM-100 and LZM-110 splicers, which utilize a  $CO_2$  laser beam as the glass heating element. The fully automated process is illustrated in Figure 8. The entire process takes less than one minute for each ball end-cap example shown in Section 3.

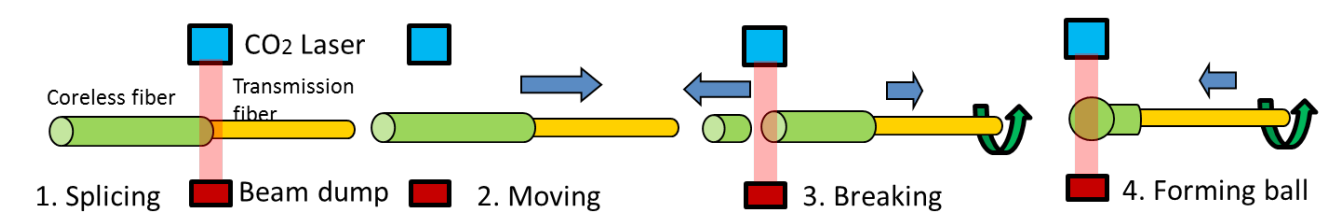


Figure 8 — The spherical end-cap manufacturing process using AFL/Fujikura LZM-100 or LZM-110 CO<sub>2</sub> laser splicers is illustrated. The splicing, fiber breaking, and the ball lensing proceed in a single continuous automated process. The ball diameter D and desired end-cap length L are all pre-calculated and preset as program parameters.

For measuring the beam quality, a typical spherical end-cap was made with Nufern 1060XP fiber ( $d_1 = 125 \,\mu\text{m}$ ,  $w_0 = 3.1 \,\mu\text{m}$ ) spliced to Nufern coreless fiber (FUD-3442,  $d_2 = 400 \,\mu\text{m}$ ). A ball end-cap with diameter  $D = 1000 \,\mu\text{m}$  and  $L = 2500 \,\mu\text{m}$  was generated. An Ophir M2-200s was used for the M² measurement at 1060 nm. The measured results are shown in Figure 9. A very good M² value (1.066) was achieved which is very close to the measurement directly from the output fiber (1.05) before splicing to the spherical end-cap.

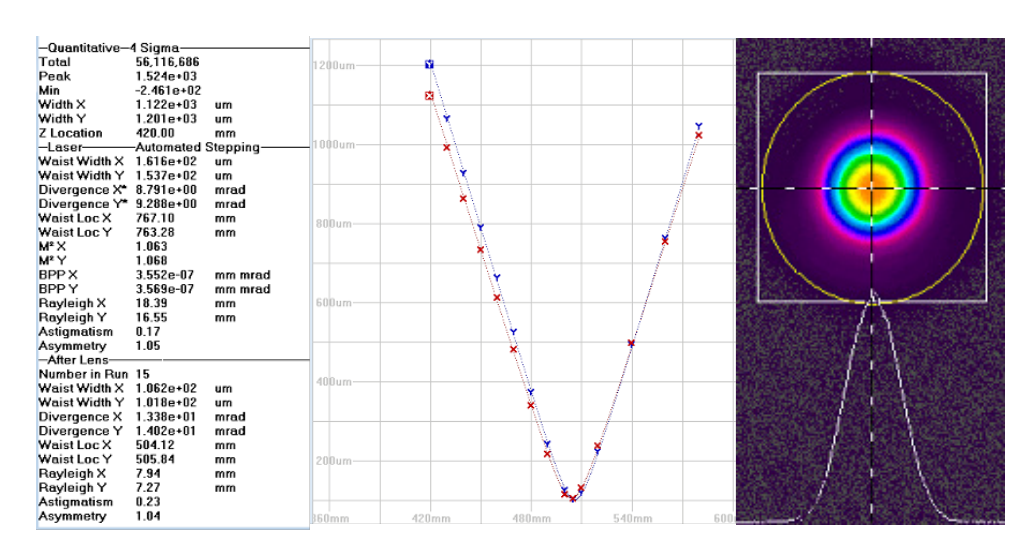


Figure 9 — Measured beam quality for spherical end-caps made with Nufern 1060XP fiber ( $d_1 = 125 \, \mu m, \, w_0 = 3.1 \, \mu m$ ) spliced to Nufern coreless fiber (FUD-3442,  $d_2 = 400 \, \mu m$ ). The ball diameter  $D = 1000 \, \mu m$  and total length  $L = 2500 \, \mu m$ . The AFL/Fujikura LZM-100 was used for making the end-cap with the process shown in Figure 8.

The beam was measured with an Ophir M2-200s at 1060 nm. The measured  $M^2$  is 1.066.



In order to make a high power test, a spherical end-cap with a large diameter D=2.2 mm was made to reduce the power density at the ball surface. The end cap material is a  $d_2=1.2$  mm coreless fused silica fiber spliced to a passive fiber of 20/400/500 µm. The total length of the end-cap is L=4.6 mm. The computed performance is  $L_{core}=-51$  dB,  $L_{clad}=-33$  dB, f=9.3 mm, and  $w_3=15$  µm without AR coating. A Convergent fiber laser system was operated at 1064 nm wavelength. A Coherent LM-5000 power head was used for propagated power measurement and a FLIR-T62101 thermal camera was used for hot spot temperature measurement. Since no AR coating and no cladding mode stripper were used, the temperature of the hottest spot at the power combiner leg was recorded and is shown in Figure 10. The temperature change is directly related to the return loss of the end-cap. The temperature comparison in Figure 10 shows very similar performance between the spherical end-caps and angle polished cylindrical end-cap. However, the manufacturing cost of spherical end-caps is much lower than that of angle polished cylindrical end-caps. The high power measurements were completed by Convergent in their lab with our appreciation.

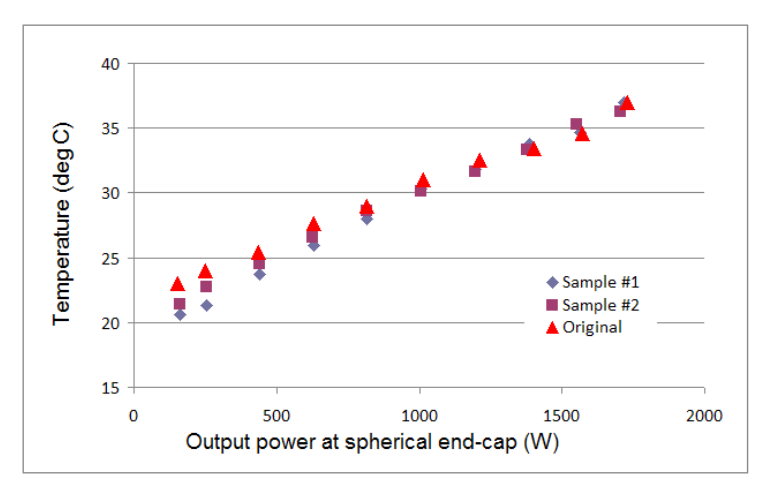


Figure 10. Sample 1 and 2 data shows measured temperatures for the spherical end-caps made with 20/400/500 LMA fiber  $(d_1 = 400 \ \mu\text{m}, \ w_0 = 9 \ \mu\text{m})$  spliced to  $d_2 = 1.2 \ \text{mm}$  coreless fiber. The uncoated ball diameter  $D = 2.2 \ \text{mm}$  and end-cap length  $L = 4.6 \ \text{mm}$ . For comparison, the data designated as "Original" shows the measured results for a cylindrical end-cap with a 5-degree polished angle.

#### 6. CONCLUSION

Ball shaped end-caps are introduced and studied in this paper. As compared to the cylindrical end-caps which are widely used in the current fiber laser industry, we found the spherical end-caps have three major benefits. First of all, the back reflection is about 10 dB to 30 dB lower than the flat uncoated cylindrical end-caps and is therefore comparable to angle polished end-caps. Secondly, ball shaped end-caps can achieve flexible beam propagation with a converging, collimated, or diverging beam shape by simply varying the design parameters L/D, where D is the ball diameter and L is the end-cap length. Finally, the manufacturing cost and time for ball shaped end-caps are much lower than that for a similar type of cylindrical end-caps.

In this paper, only the fundamental mode was considered for fiber laser systems using SMF or LMA as the output fiber. For spherical end-caps developed for multimode output fibers, the discussion will be continued in a separate paper.

## **ACKNOWLEDGEMENTS**

The authors wish to thank Doug Duke for providing proofreading to the article, Brad Hendrix for market analysis, and Al Swanson for his support to the project.



#### **REFERENCES**

- 1. Limpert, J., Roser, F., Schreiber, T., and Tunnermann, A., "High-power ultrafast fiber laser systems," IEEE JSTQE, vol. 12, no. 2, March/April, 2006.
- 2. Wallace, J., "Material processing: 100 kW fiber laser, power meter serve industry," Laser Focus World, Dec. 6th, 2013, <a href="https://www.laserfocusworld.com/articles/print/volume-49/issue-12/world-news/materials-processing-100-kw-fiber-laser-power-meter-serve-industry.html">https://www.laserfocusworld.com/articles/print/volume-49/issue-12/world-news/materials-processing-100-kw-fiber-laser-power-meter-serve-industry.html</a>
- **3.** Fiberguide, "End Capped High Power Assemblies," 2014, <a href="https://www.fiberguide.com/wp-content/uploads/2014/01/End-Capdatasheet-01-20-14.pdf">https://www.fiberguide.com/wp-content/uploads/2014/01/End-Capdatasheet-01-20-14.pdf</a>
- **4**. Zheng, W., "Optic Lenses Manufactured on Fiber Ends," Optoelectronics Global Conference (2015), <a href="http://ieeexplore.ieee.org/document/7336855/">http://ieeexplore.ieee.org/document/7336855/</a>. <a href="http://ieeexplore.ieee.org/document/733685/">h
- **5**. Boehme, S., Beckert, E., Eberhardt, R., and Tuennermann A., "Laser splicing of end caps: process requirements in high power laser applications," Proceedings of SPIE The International Society for Optical Engineering, Proc. of SPIE Vol. 7202 720205-1, February 2009.
- **6**. Wetter, A., Faucher, M., Sévigny, B., and Vachon, N., "High core & cladding isolation termination for high power lasers and amplifiers," Proceedings of the SPIE, Volume 7195, id. 719521 (2009).
- 7. Lyngnes, O., Ode, A., and Ness, D., "Anti Reflection Coating Damage Threshold Dependence on Substrate Material," <a href="http://www.precisionphotonics.com">http://www.precisionphotonics.com</a>
- 8. Zhou, X., Chen, Z., Wang, Z., and Hou, J., "Monolithic fiber end cap collimator for high-power free-space fiber—fiber coupling," Applied Optics, Vol. 55, No. 15, May, 2016



www.AFLglobal.com